INVESTIGATIONS OF PHASE TRANSITIONS IN $(NH_4)_3H(SO_4)_2$ CRYSTAL BY MEANS OF Mn^{2+} EPR SPECTRA

W. BEDNARSKI AND S. WAPLAK

Institute of Molecular Physics, Polish Academy of Sciences
Smoluchowskiego 17/19, 60-179 Poznań, Poland

(Received June 11, 1996; revised version September 9, 1996)

EPR of Mn^{2+} impurity ion in the $(NH_4)_3H(SO_4)_2$ crystal is studied in the temperature range 80–420 K. It is shown that Mn^{2+} substitutes NH_4^+(I) ion and is coordinated in deformed oxygen octahedron in which takes two "off-center" positions. Its spin-Hamiltonian parameters and direction cosines of crystal field are determined. The successive EPR line splitting for three phase transitions is discussed.

PACS numbers: 61.50.–f, 76.30.–v

1. Introduction

Tri-ammonium hydrogen disulphate $(NH_4)_3H(SO_4)_2$ is the member of the X_3ZY_2 crystals family (X = NH_4 or alkali metal, Z = H, D; Y = SO_4, SeO_4). They have been found to exhibit ferroelastic properties, but only compounds containing ammonium groups NH_4^+ have complex phase diagrams and ferroelectric properties order under certain conditions [1–3].

At atmospheric pressure 5 successive phase transitions at temperatures of 413 K, 265 K, 140 K, 136 K and 78 K were known in the $(NH_4)_3H(SO_4)_2$ (TAHS) until 1994 year. The six phases are denoted as I, II, III, IV, V and VII respectively. According to [4] there exists one more phase transition at about 463 K visible as a sudden jump in conductivity value at c^* direction.

This paper deals with the Mn^{2+} EPR spectrum in TAHS at room temperature (RT) and its temperature evolution.

The Mn^{2+} with ionic radius $r(Mn^{2+}) = 0.91$ Å which replaces NH_4^+ with ionic radius $r(NH_4^+) = 1.47$ Å may introduce only small lattice disturbance. Simultaneously, the presence of fine and hyperfine EPR structure for Mn^{2+} ($S = 5/2$, $I = 5/2$) makes this probe more sensitive for phase transitions. It is why we used Mn^{2+} EPR spectra for especially subtle phase transitions II–III with suggested incommensurability and II–I with superprotonic properties.

2. Experimental procedure

Single crystals of TAHS were grown by slow evaporation at 303 K, of an aqueous solution containing 40.6 wt% of $(NH_4)_2SO_4$ and 24.0 wt% of H_2SO_4. In addition 2 wt% of $MnSO_4 \cdot 4H_2O$ was added to mother solution leading to real Mn^{2+} concentration in crystal of order 10 ppm like that studied by Suresh Babu et al. [5]. The crystals grown were pseudo-hexagonal with predominant (001) planes.

The Mn^{2+} EPR spectrum was studied in the range of 80–450 K by using SE/X 2343 spectrometer. Investigations were carried out in 3-cm wavelength region (X-band). The temperature achieved by blowing the nitrogen vapors through a quartz dewar with the sample positioned in the resonance cavity was controlled by means of copper–constantan thermocouple and 650H (UNIPAN) temperature controller with ±0.5 K accuracy.

3. Spin-Hamiltonian parameters and coordination of Mn^{2+} in TAHS at room temperature

The orthogonal coordinate system XYZ chosen for EPR anisotropy pattern was related to the monoclinic symmetry of crystallographic axes a, b of a single-domain crystal in phase II as follows: $\boldsymbol{X} \parallel a$, $\boldsymbol{Y} \parallel b$, $\boldsymbol{Z} \parallel c^* = a \times b$.

We have analysed the EPR spectrum of Mn^{2+} doped TAHS at RT with the spin-Hamiltonian for ions in monoclinic symmetry [6, 7]:

$$H = \beta \boldsymbol{B} \boldsymbol{g} \boldsymbol{S} - B_4(O_4^0 + 20\sqrt{2}O_4^3) + B_2^0 O_2^0 + B_4^0 O_4^0 + A_{xx} S_x I_x + A_{yy} S_y I_y + A_{zz} S_z I_z, \tag{1}$$

where O_n^m — spin operators, B_n^m — crystal field parameters, A_{ii} — hyperfine structure components, β — Bohr magneton, g — spectroscopic tensor.

According to [7], for the main crystal field gradient V_{zz} parallel to an external magnetic field B, the EPR spectrum for different electron transitions can be described by the following equations:

$$|\pm 5/2, m\rangle \Leftrightarrow |\pm 3/2, m\rangle$$

$$B = B_0 \mp 4D \pm (4/3)(a - F) + 4E^2/B_0 - A_{\parallel} m - A_{\perp}^2 (35/4 - m^2 \pm 4m)/2B_0, \tag{2}$$

$$|\pm 3/2, m\rangle \Leftrightarrow |\pm 1/2, m\rangle$$

$$B = B_0 \mp 2D \mp (5/3)(a - F) + 5E^2/B_0 - A_{\parallel} m - A_{\perp}^2 (35/4 - m^2 \pm 2m)/2B_0, \tag{3}$$

$$|+1/2, m\rangle \Leftrightarrow |-1/2, m\rangle$$

$$B = B_0 - 8E^2/B_0 - A_{\parallel} m - A_{\perp}^2 (35/4 - m^2)/2B_0, \tag{4}$$

where g is the spectroscopic factor; $B_0 = h\nu/\beta g$; D, E, a, F — crystal field parameters; $A_{\parallel}$ and $A_{\perp}$ — components of hyperfine structure tensor $\boldsymbol{A}$. The relations between crystal field parameters used in Eq. (1) and Eqs. (2)–(4) are: $a = 120B_4$, $D = 3B_2^0$, $F = 180B_4^0$ and $E = B_2^2$. Equations (2)–(4) are correct if one assumes isotropy of g-factor and axiality of $\boldsymbol{A}$ tensor ($A_{zz} = A_{\parallel}$, $A_{xx} = A_{yy} = A_{\perp}$).

The EPR spectrum of single-domain crystal shows at RT two types of complexes, denoted as $Mn^{2+}(1)$ and $Mn^{2+}(2)$, similarly as it has been found for VO^{2+} ions doped $(NH_4)_3H(SO_4)_2$ monocrystals [8–10]. Only one complex of Mn^{2+} has

TABLE I

Parameters of spin-Hamiltonian of $Mn^{2+}(1)$ and $Mn^{2+}(2)$ centers in $(NH_4)_3H(SO_4)_2$ crystals at room temperature (295 K).

Center	Parameter					
	D [Gs]	E [Gs]	$a-F$ [Gs]	g	$A_\parallel$ [Gs]	$A_\perp$ [Gs]
$Mn^{2+}(1)$	500 ± 5	62 ± 3	-2 ± 3	1.993 ± 0.005	-91.3 ± 1.0	-94.9 ± 1.0
$Mn^{2+}(2)$	498 ± 5	62 ± 3	0 ± 3	1.993 ± 0.005	-92.5 ± 1.5	-94.6 ± 1.1

TABLE II

Direction cosines two types of Mn^{2+} ions in TAHS:Mn^{2+} at RT.

Center	Main axes of the complex	Direction cosines		
		X	Y	Z
$Mn^{2+}(1)$	x_1	± 0.891	$+0.256$	∓ 0.375
	y_1	∓ 0.416	$+0.791$	∓ 0.450
	z_1	± 0.182	$+0.556$	± 0.811
$Mn^{2+}(2)$	x_2	± 0.424	-0.819	± 0.358
	y_2	± 0.842	$+0.216$	∓ 0.495
	z_2	± 0.334	$+0.511$	∓ 0.792

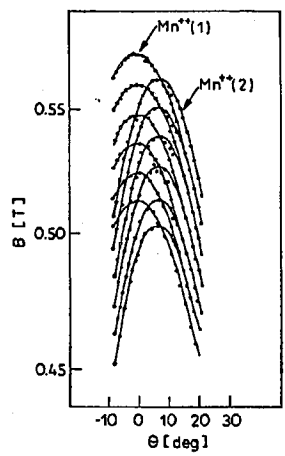

Fig. 1. Angular dependence of the lines position near z_1 axis in z_1x_1 plane for electron transitions $|-5/2, m\rangle \Leftrightarrow |-3/2, m\rangle$ at RT: • experimental points; —— fit.

been described in paper [5]. The spin-Hamiltonian parameters as well as direction cosines for both Mn^{2+} centers in TAHS are given in Tables I and II.

Figure 1 shows a part of anisotropy in z_1x_1 plane. There are two possible positions for Mn^{2+} ions in the crystal lattice (Fig. 2):

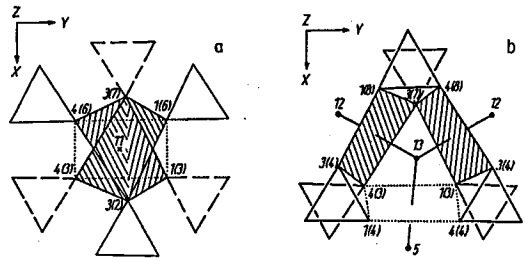

Fig. 2. Nearest possible neighborhoods of Mn^{2+} ion (reprinted from [10]) in monoclinic phase II: (a) replacing NH_4^+(I) ion denoted as 11; (b) occupying an interstitial position between vacancies of NH_4^+(II) ions denoted as 5, 12 and 13. Three possible coordination planes are indicated and SO_4 groups are marked by triangles. Nearest to Mn^{2+} oxygen atoms are denoted as $m(n)$, where m-th oxygen belongs to n-th sulphur.

(a) NH_4^+(I) vacancy position which is the special position at the axis of twofold symmetry;

(b) an interstitial position between two vacancies of the nearest NH_4^+(II) ions.

The crystal field parameters evaluated from Eqs. (2)–(4) indicate that the both centers take the same coordination position. The EPR studies of the effect of ferroelastic switching (6 centers in ferroelastic 3-domain crystal) show that in case (b) it requires diffusion of the Mn^{2+} to a distance about 3 Å. We believe that case (a) is the most realistic because reorientation of Z-axis alone would suffice to provide three kinds of coordination with six nearest oxygens. The presence of two types $Mn^{2+}(1)$ and $Mn^{2+}(2)$ ions in the studied monodomain crystals can be explained as being due to occupation of two noncentral, energetically inequivalent positions within the same coordination environment.

4. Temperature dependence of the Mn^{2+} spectra below RT phase transitions

We had described earlier the behavior of the Mn^{2+} complexes in II–III transition and phase III [11]. Detailed analysis of the δB splitting of each Mn^{2+} line below $T_c^{II} \approx 265$ K indicates that TAHS undergoes second-order phase transition at about 265 K. This splitting appears to be proportional to the order parameter with its small sinusoidal type of modulation. Similar effect was also observed by us for SeO_3^- radicals doped $(NH_4)_3H(SO_4)_2$ monocrystals [11].

Such order parameter temperature behavior suggests that phase III is a modulated structure and paramagnetic impurities reflect phase fluctuation in pure crystal [11]. This statement is supported by X-ray studies [12], where the critical diffuse scattering was shown near T_c^{II}. Authors of this investigation indicated that the crystalline phase III has incommensurate modulation characterized by satellite reflections.

The reorientation of SO_4^{2-} (coordinational surrounding of Mn^{2+} impurities) and NH_4^+ ions in phase III is confirmed by detected differences in the main crystal field directions of complexes denoted as $Mn^{2+}(1a)$ and $Mn^{2+}(1b)$ which is presented in Fig. 3. EPR lines $Mn^{2+}(1a)$ and $Mn^{2+}(1b)$ appear as a result of

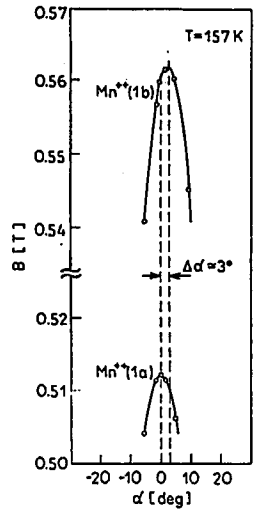

Fig. 3. Angular dependence of the EPR lines position belonging to $Mn^{2+}(1a)$ and $Mn^{2+}(1b)$ complexes near y_1 axis in x_1y_1 plane for electron transition $|-5/2, -5/2\rangle \Leftrightarrow |-3/2, -5, 2\rangle$ at 157 K.

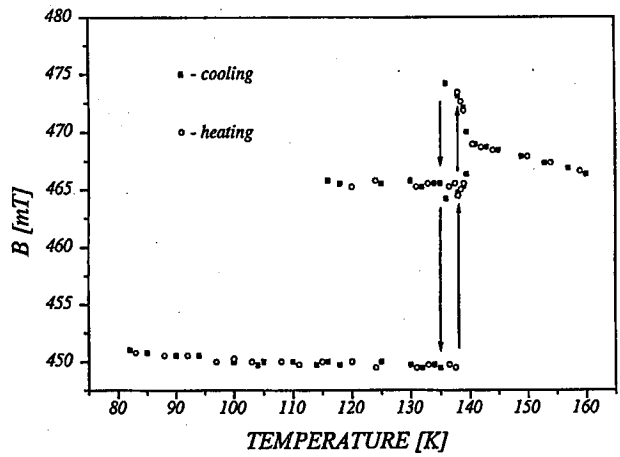

Fig. 4. Temperature evolution of the line position of $Mn^{2+}(1b)$ center for electron $|-5/2, -5/2\rangle \Leftrightarrow |-3/2, -5/2\rangle$ transition. The arrows indicate an abrupt change in line positions.

$Mn^{2+}(1)$ line splitting below temperature 265 K. The difference of $\Delta\alpha$ orientation for the mentioned above centers in x_1y_1 plane is equal to about 3 degrees at 157 K.

Figure 4 shows the changes in positions and splitting of $Mn^{2+}(1b)$ EPR line below 160 K for electron transition $|-5/2, -5/2\rangle \Leftrightarrow |-3/2, -5/2\rangle$. At $T_c^{III} =$ 140 K there is a gradual line splitting which proves that III–IV phase transition

is of the second order. With the temperature lowering we observe discontinuous changes in positions of splitted lines at $T_c^{IV} \approx 135$ K, and below about 115 K one of them disappears. After heating this line appears again but now abrupt changes in positions of the EPR lines alternate at $T_c^{IV'} \approx 138$ K. The difference in T_c^{IV} and $T_c^{IV'}$ corresponds to thermal hysteresis observed by dielectric study [13].

5. EPR in ferroelastic II and superprotonic I phases

Tri-ammonium hydrogen disulphate transforms from ferroelastic monoclinic ($A2/a$) phase II to paraelastic trigonal ($R\text{-}3m$) [14] with superprotonic properties [15] at 413 K. The symmetry of Mn^{2+} EPR spectrum at RT (Table I) is consistent with monoclinic symmetry of TAHS for which the crystal field parameter E in Eqs. (2)–(4) is not equal to 0. The difference between $Mn^{2+}(1)$ and $Mn^{2+}(2)$ orientation disappears with temperature increasing and linewidth grows up as shown in Fig. 5.

At 401 K one can see abrupt line width decrease which in our opinion indicates the phase transition II–I. This conclusion is supported by the fact that

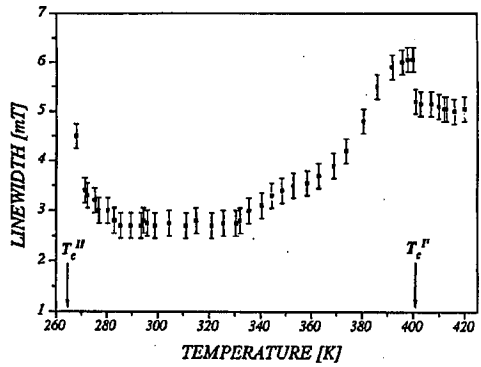

Fig. 5. The EPR linewidth of $Mn^{2+}(1)$ versus temperature for electron transition $|\pm 3/2, m\rangle \Leftrightarrow |\pm 1/2, m\rangle$.

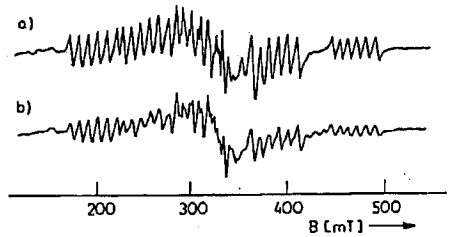

Fig. 6. EPR spectra recorded at 295 K for crystal $(NH_3)H(SO_4)_2 : Mn^{2+}$: (a) before heating a monodomain sample above the temperature of II–I phase transition; (b) after recooling a crystal from $T \approx 410$ K.

above $T_c^{I'} = 401$ K in doped $(NH_4)_3H(SO_4) : Mn^{2+}$ the EPR spectrum consists of lines characteristic of one complex in axial symmetry of crystal field ($E = 0$).

After crystal recooling from $T > T_c^{I'}$ to RT the changes in the EPR spectrum of a monodomain sample were recorded. Figure 6 presents EPR spectra recorded at 295 K before (a) and after (b) heating TAHS to the temperature 410 K. Additional lines visible in Fig. 6b belong to another domain created in phase transition I–II. This indicates that monodomain crystal became multidomain one.

The trigonal symmetry of phase I admits three directions of distortion differing by 120° in the XY plane signifying that, below T_c^I, the crystal can occur in three distinct states of orientation (three ferroelastic domains) [16]. In general, one can say that the EPR spectra will exhibit the symmetry of the high-temperature phase in specimens which contain all three kinds of domains and will represent a superposition of the spectra of one-domain specimens, oriented in accordance with the possible directions of distortion of the initial phase.

6. Discussion

In the $(NH_4)_3H(SO_4)_2 : Mn^{2+}$ two types of Mn^{2+} complexes exist at room temperature (ferroelastic phase II). The differences in orientations of main axes and the identical spin-Hamiltonian parameters of both ions suggest that the impurities occupy the same coordination environment. The position presented in Fig. 2a seems to be more realistic, since it permits a straightforward interpretation of the considerable reorientation of Mn^{2+} in phase transition II–I.

Consequently, in the case of doped crystals, below $T_c^{I'} = 401$ K the Mn^{2+} ions occupy two noncentral positions and are slightly displaced from a NH_4^+ vacancy. Above II–I transition the mentioned positions are thermally averaged and we observe only one axial complex. Such a model of two types of Mn^{2+} is confirmed by the fact that the ionic size of impurity is smaller than the ionic radius of NH_4^+ group. The temperature study shows that all phase transitions are conspicuous by the EPR spectrum.

The lowering of the temperature transition I–II from 413 K in case of pure crystal to 401 K for doped samples is probably coupled with vacancies which are created to compensate an extra electric charge introduced by admixture itself.

As it has been shown for isomorphic $K_3H(SO_4)_2$ (KHS) doped with Mn^{2+} or VO^{2+} [17] ions there is no defect influence on the transition temperature to superprotonic phase at $T = 471$ K. The main role in conductivity below about 380 K is played by a proton–vacancy movement inside $(SO_4–H...SO_4)^{3-}$ dimers and among next-nearest dimers. Above 380 K proton diffusion involving distant dimers is activated.

In accordance with proton conductivity model in TAHS [15] proton vacancies are produced in the $(NH_4)^+$ sublattice and proton is transferred to SO_4^{2-} to form HSO_4^-. Hence conduction takes place through the proton transfer along the chains of the N–H...O form. If this model is correct, then impurities decrease the potential barriers in hydrogen bonded $H_3N–H...O–SO_3$ chains leading to T_c^I decreasing.

Inhomogeneous order parameter fluctuation at phase III observed by Mn^{2+} EPR line splitting is due to incommensurate modulation confirmed by other methods [12, 18], although until now there is no adequate theoretical description of this

fluctuation. The earlier EPR data driven from VO^{2+} and SeO_3^- paramagnetic centers in $(NH_4)_3H(SO_4)_2$ [9,10] show the successive unit cell doubling recorded at phase transitions. These data are fully reproducible in Mn^{2+} spectra as well.

References

[1] K. Gesi, *J. Phys. Soc. Jpn.* **48**, 886 (1980).

[2] J. Minge, Ph.D. Thesis, Poznań 1985.

[3] K. Gesi, *Jpn. J. Appl. Phys.* **19**, 1051 (1980).

[4] T. Fukami, K. Tobaru, K. Kaneda, K. Nakasone, K. Furukawa, *J. Phys. Soc. Jpn.* **63**, 2006 (1994).

[5] D. Suresh Babu, G.S. Sastry, M.D. Sastry, A.G. Dalvi, *J. Phys. C, Solidi State Phys.* **18**, 6111 (1985).

[6] A. Abragam, B. Blaney, *Electron Paramagnetic Resonance of Paramagnetic Ions*, Claredon Press, Oxford 1970.

[7] R. Hrabański, Ph.D. Thesis, Poznań 1980.

[8] J. Minge, S. Waplak, L. Szczepańska, *Acta Phys. Pol. A* **64**, 151 (1983).

[9] M. Fujimoto, B.V. Sinha, *Ferroelectrics* **46**, 227 (1983).

[10] J. Minge, S. Waplak, *Phys. Status Solidi B* **123**, 27 (1984).

[11] S. Waplak, W. Bednarski, *Mol. Phys. Rep.* **9**, 97 (1995).

[12] S. Suzuki, M. Takahashi, Y. Makita, K. Gesi, *Meeting of the Physical Society of Japan*, Yamagata Univ., 1976.

[13] K. Gesi, *Phys. Status Solidi A* **33**, 479 (1976).

[14] S. Suzuki, *J. Phys. Soc. Jpn.* **47**, 1205 (1979).

[15] A. Devendar Reddy, S.G. Sathyanarayan, G. Sivarama Sastry, *Solid State Commun.* **43**, 937 (1982).

[16] K. Aizu, *J. Phys. Soc. Jpn.* **28**, 704 (1970).

[17] S. Waplak, *Acta Phys. Pol. A* **89**, 939 (1994).

[18] S. Suzuki, Y. Oshino, K. Gesi, *J. Phys. Soc. Jpn.* **47**, 874 (1979).